

# On the generation of solitons and breathers in the modified Korteweg–de Vries equation

Simon Clarke, Roger Grimshaw, and Peter Miller

*Department of Mathematics and Statistics, Monash University, Clayton, Victoria, Australia*

Efim Pelinovsky and Tatiana Talipova

*Institute of Applied Physics and Nizhny Novgorod Technical University, Nizhny Novgorod, Russia*

(Received 19 October 1999; accepted for publication 28 March 2000)

We consider the evolution of an initial disturbance described by the modified Korteweg–de Vries equation with a positive coefficient of the cubic nonlinear term, so that it can support solitons. Our primary aim is to determine the circumstances which can lead to the formation of solitons and/or breathers. We use the associated scattering problem and determine the discrete spectrum, where real eigenvalues describe solitons and complex eigenvalues describe breathers. For analytical convenience we consider various piecewise-constant initial conditions. We show how complex eigenvalues may be generated by bifurcation from either the real axis, or the imaginary axis; in the former case the bifurcation occurs as the unfolding of a double real eigenvalue. A bifurcation from the real axis describes the transition of a soliton pair with opposite polarities into a breather, while the bifurcation from the imaginary axis describes the generation of a breather from the continuous spectrum. Within the class of initial conditions we consider, a disturbance of one polarity, either positive or negative, will only generate solitons, and the number of solitons depends on the total mass. On the other hand, an initial disturbance with both polarities and very small mass will favor the generation of breathers, and the number of breathers then depends on the total energy. Direct numerical simulations of the modified Korteweg–de Vries equation confirms the analytical results, and show in detail the formation of solitons, breathers, and quasistationary coupled soliton pairs. Being based on spectral theory, our analytical results apply to the entire hierarchy of evolution equations connected with the same eigenvalue problem. © 2000 American Institute of Physics. [S1054-1500(00)01202-7]

**The modified Korteweg–de Vries equation describes nonlinear wave propagation in many physical systems with polarity symmetry. The fundamental nonradiating solutions of this equation with a positive coefficient for the nonlinear term are solitons and breathers. These correspond, respectively, to discrete eigenvalue pairs and eigenvalue quartets for the associated scattering problem. Here we consider a class of piecewise-constant initial conditions, using analytical and numerical solutions of the scattering problem and direct numerical simulations of the modified Korteweg–de Vries equation. We demonstrate that initial conditions with large mass and energy favor the formation of solitons, while those with small mass, but finite energy favor the formation of breathers. Our results admit immediate generalization to many other integrable equations.**

many branches of physics when there is polarity symmetry. For instance, applications in the context of electrodynamics are described by Perelman *et al.* in Ref. 1, in the context of wave propagation in size-quantized films by Pelinovsky and Sokolov in Ref. 2, in the context of stratified fluids by several authors in Ref. 3 and Ref. 4, and finally in the context of elastic media by Pavlov in Ref. 5. Equation (1), like the Korteweg–de Vries equation, is integrable, and can be solved by the inverse scattering method (see, for example, Lamb,<sup>6</sup> Dodd *et al.*<sup>7</sup> or Drazin and Johnson<sup>8</sup>). As is well-known, the steady-state, bounded traveling-wave solution of this equation is a *soliton* of either polarity

$$u = A \operatorname{sech}[A(x - A^2t - x_0)], \quad (2)$$

where  $A$  is the soliton amplitude, and  $x_0$  is an arbitrary phase. The *polarity* of the soliton refers to the sign of  $A$ . It is important to note that the mass of a soliton is fixed,

$$M_s = \int_{-\infty}^{+\infty} u(x) dx = \pi \operatorname{sign} A, \quad (3)$$

and does not depend on the soliton amplitude. Multisoliton solutions can be found by several methods: the inverse scattering method, the Hirota bilinear formalism, or Bäcklund–Darboux transformations. Within the “complexification” of the family of two-soliton solutions obtained by any of these methods, one finds the other elementary excitations of the

## I. INTRODUCTION

The modified Korteweg–de Vries equation with a positive coefficient for the cubic nonlinear term,

$$\frac{\partial u}{\partial t} + 6u^2 \frac{\partial u}{\partial x} + \frac{\partial^3 u}{\partial x^3} = 0, \quad (1)$$

here presented in standard form, is well-known as a canonical model for the description of nonlinear long waves in

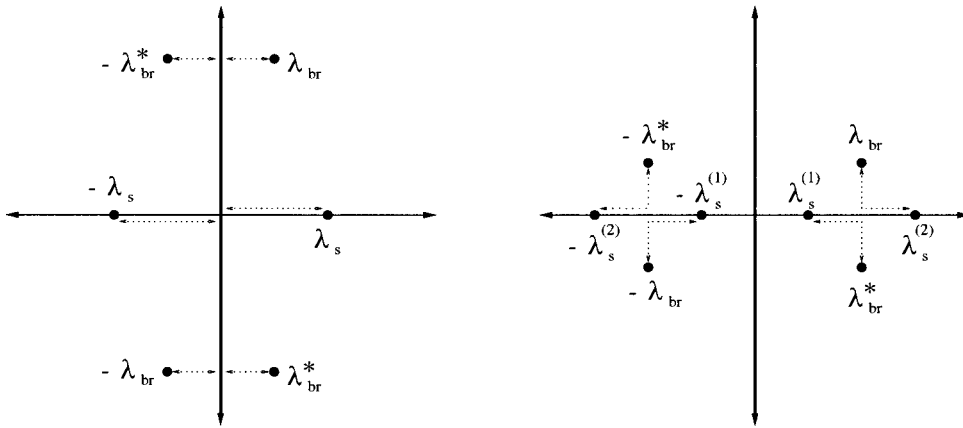


FIG. 1. Possible bifurcations of the discrete spectrum for the AKNS eigenvalue problem (5). Left: the bifurcations of breather eigenvalue quartets and soliton eigenvalue pairs to and from the continuous spectrum on the imaginary axis. The continuous spectrum is the imaginary  $\lambda$ -axis, indicated in bold. Right: the splitting of a breather into two solitons, or the merging of two solitons to form a breather.

modified Korteweg–de Vries equation—the *breathers*. An isolated breather is a solution of (1) of the form

$$u = -4\alpha \operatorname{sech} \theta \cdot \left[ \frac{\cos \phi + (\alpha/\beta) \sin \phi \cdot \tanh \theta}{1 + (\alpha/\beta)^2 \sin^2 \phi \operatorname{sech}^2 \theta} \right], \quad (4)$$

where  $\theta = -2\beta x - 8\beta(\beta^2 - 3\alpha^2)t + \theta_0$ ,  $\phi = 2\alpha x + 8\alpha(3\beta^2 - \alpha^2)t + \phi_0$ , and where  $\alpha$ ,  $\beta$ ,  $\theta_0$ , and  $\phi_0$  are arbitrary real parameters. Breathers are sometimes called “oscillatory pulse solitons” because although they are isolated disturbances propagating without any loss, they have internal oscillatory degrees of freedom, and are not traveling waves of permanent form *per se*. Due to these internal degrees of freedom, small amplitude breathers are very difficult to distinguish in practice from dispersive radiation components of the solution of (1) over fixed time intervals of observation. All breather solutions have zero mass, so that  $M_{br} = 0$ .

Because the solitons and breathers are the fundamental nondispersive excitations of the modified Korteweg–de Vries equation, our aim in this article is to develop an understanding of what classes of initial conditions for (1) lead to the formation of solitons and/or breathers. We are aware of only one totally analytical result in this context (by “totally analytical” we mean here that not only can an analytical eigenvalue condition be obtained in the form of an implicit relation, but also that the relation can be solved explicitly in closed form), namely the study by Satsuma and Yajima,<sup>9</sup> which showed (essentially) that a “soliton-like” initial disturbance [i.e., proportional to  $\operatorname{sech}(x)$ ] for the modified Korteweg–de Vries equation generates solitons and an oscillatory tail, but no breathers; for the generation of solitons it is further necessary to have an initial disturbance with mass greater than  $\pi/2$ . Here we will study the process of soliton and breather generation from various initial disturbances, represented by piecewise-constant functions for analytical convenience, and by similar (slightly smoothed) functions in our direct numerical simulations of the initial value problem for (1).

## II. EIGENVALUES OF THE SCATTERING PROBLEM

Equation (1) is integrable, and the initial-value problem can be solved by the inverse scattering method. Here we use the Ablowitz-Kaup-Newall-Segur (AKNS) scheme (see, for instance, Drazin and Johnson<sup>8</sup>),

$$\begin{aligned} \frac{\partial \varphi_1}{\partial x} &= -u(x)\varphi_2 + \lambda\varphi_1, \\ \frac{\partial \varphi_2}{\partial x} &= +u(x)\varphi_1 - \lambda\varphi_2, \end{aligned} \quad (5)$$

where  $u(x)$  is an initial disturbance for the modified Korteweg–de Vries equation (1), and  $\lambda$  is the (generally complex-valued) eigenvalue. Here we assume that  $u(x)$  is localized, that is, it decays rapidly as  $|x| \rightarrow \infty$ ; in fact, in our analytical work  $u(x)$  will vanish identically outside a finite domain. The reader should note that in the literature, a “90°-rotated” version of the spectral parameter more commonly appears, in which case (5) is written in terms of  $\zeta = i\lambda$ . The fact that the scattering problem (5) is used to solve many other physically important equations (e.g., the nonlinear Schrödinger equation, the sine-Gordon equation, the undamped Maxwell–Bloch equations, etc.) means that all results we will obtain here for the modified Korteweg–de Vries equation imply analogous results for these equations as well.

The spectrum of (5) consists of the continuous spectrum on the whole imaginary  $\lambda$ -axis, and a number of discrete eigenvalues for which there exists a solution of (5) with  $\varphi_1(x)$  and  $\varphi_2(x)$  being functions that decay as  $|x| \rightarrow \infty$ . While the discrete spectrum eigenvalues must have nonzero real parts, they may emerge from certain spectral singularities in the continuous spectrum as a parameter is varied. We will see examples of this below. Elementary symmetries of (5) that follow from the reality of the potential  $u(x)$  imply that whenever  $\lambda$  is an eigenvalue, then so are  $\lambda^*$ ,  $-\lambda$ , and  $-\lambda^*$ . This means that the nonimaginary eigenvalues of (5) either come in pairs  $(\lambda_s, -\lambda_s)$  for  $\lambda_s$  real, or in quartets  $(\lambda_{br}, -\lambda_{br}^*, -\lambda_{br}, \lambda_{br}^*)$  for  $\lambda_{br}$  genuinely complex. Without loss of generality, in the former case we assume that  $\lambda_s > 0$ , while in the latter case we assume that  $\lambda_{br}$  is in the first

quadrant of the complex  $\lambda$ -plane. Then, the possible bifurcations that can occur in the discrete spectrum as a parameter in the potential is varied are limited to the birth of breather eigenvalue quartets and soliton eigenvalue pairs from the continuous spectrum as illustrated in Fig. 1 on the left, and the coalescence of breather eigenvalue quartets on the real axis giving rise to two distinct soliton eigenvalue pairs, as illustrated in Fig. 1 on the right.

Our main concern is with the discrete spectrum, which can be found by assuming  $\mathcal{R}(\lambda) > 0$  and  $\mathcal{I}(\lambda) \geq 0$  (to single out a representative of each eigenvalue pair and quartet), and requiring that the functions  $\varphi_1(x; \lambda)$  and  $\varphi_2(x; \lambda)$  vanish at infinity. We are primarily concerned with the discrete spectrum because each pair and quartet of eigenvalues encoded in the potential  $u(x)$  yields a ‘‘permanent’’ contribution to the solution of the modified Korteweg–de Vries equation (1) for the initial data  $u(x, 0) = u(x)$ . Namely, each real pair of eigenvalues corresponds to a soliton (2) with amplitude given by  $|A| = 2\lambda_s > 0$ , while each complex quartet of eigenvalues corresponds to a breather (4) with  $\lambda_{br} = \alpha + i\beta$ . While the polarity and position of each soliton, and likewise the values of the phase constants  $\theta_0$  and  $\phi_0$  for each breather, are not determined by the eigenvalue, they are indeed given by certain auxiliary spectral data connected with the eigenfunctions  $\varphi_1(x)$  and  $\varphi_2(x)$  that we do not discuss here.

There may be other, transient, contributions to the solution of (1) with initial data  $u(x, 0) = u(x)$ . These contributions concern the formation of a dispersive oscillatory tail in  $u(x, t)$  and their presence is indicated in the initial data  $u(x)$  by a continuous spectrum reflection coefficient for (5) that does not vanish identically as a function of purely imaginary  $\lambda$ . Because these are transient effects, the detailed study of the scattering problem (5) for pure imaginary  $\lambda$  is of less direct importance for the long-time behavior of  $u(x, t)$  than the study of the discrete spectrum. There is, however, one quantity that is very useful to calculate for imaginary  $\lambda$  with the aim of determining the number of discrete eigenvalues in the right half-plane (and hence in the left half-plane by symmetry). This is the reciprocal of the transmission coefficient  $a(\lambda) = 1/T(\lambda)$  defined for pure imaginary  $\lambda$  by considering the two solutions  $(\varphi_1^\pm(x; \lambda), \varphi_2^\pm(x; \lambda))^T$  of (5) defined by the boundary conditions

$$\begin{aligned} \begin{pmatrix} \varphi_1^+(x; \lambda) \\ \varphi_2^+(x; \lambda) \end{pmatrix} \exp(\lambda x) &\rightarrow \begin{pmatrix} 0 \\ 1 \end{pmatrix}, & x \rightarrow +\infty, \\ \begin{pmatrix} \varphi_1^-(x; \lambda) \\ \varphi_2^-(x; \lambda) \end{pmatrix} \exp(-\lambda x) &\rightarrow \begin{pmatrix} 1 \\ 0 \end{pmatrix}, & x \rightarrow -\infty, \end{aligned} \tag{6}$$

and setting

$$a(\lambda) = \varphi_1^-(x; \lambda) \varphi_2^+(x; \lambda) - \varphi_2^-(x; \lambda) \varphi_1^+(x; \lambda). \tag{7}$$

This function is independent of  $x$  and is defined *ab initio* for purely imaginary  $\lambda$ , but in fact can be shown to have an analytic continuation into the right half-plane, where it satisfies  $a(\lambda) \rightarrow 1$  as  $\lambda \rightarrow \infty$  [in any direction with  $\mathcal{R}(\lambda) > 0$ ]. The zeros of its analytic continuation for  $\mathcal{R}(\lambda) > 0$  correspond exactly to the discrete eigenvalues of (5) lying in the right half-plane. While this analytic continuation procedure is not always how one seeks the eigenvalues in practice, it

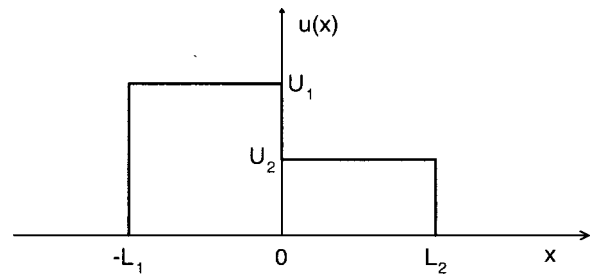


FIG. 2. An initial disturbance of rectangular well form.

follows from the argument principle for complex functions that the *index* of the function  $a(\lambda)$  for  $\mathcal{R}(\lambda) = 0$ , defined as the number of times the phase of  $a(\lambda)$  increases by  $2\pi$  as  $\lambda$  varies continuously from  $-i\infty$  to  $i\infty$ , is exactly the number of eigenvalues of (5) in the right half-plane. It is sometimes convenient to use parametric plots of the curve  $[\mathcal{R}(a(\lambda)), \mathcal{I}(a(\lambda))]$  to determine the total number of excitations to expect; we first encountered such plots in the article of Lewis.<sup>10</sup> From these plots the number of eigenvalues in the right half-plane is then given by the integral

$$N = -\frac{1}{2\pi i} \int_{-i\infty}^{+i\infty} \frac{a'(\lambda)}{a(\lambda)} d\lambda. \tag{8}$$

Although an unstable numerical calculation for general initial data, for initial data having compact support it is not at all difficult to construct numerically  $a(\lambda)$  for  $\mathcal{R}(\lambda) > 0$  directly. Then, a similar index integral can then be used to obtain the number of discrete eigenvalues lying on the positive real axis, which is the number of solitons which evolve from the initial disturbance. Let  $\Gamma$  be the counterclockwise-oriented perimeter of a vanishingly thin but infinitely long rectangle enclosing the positive real axis. Then the total number of solitons is

$$N_s = \frac{1}{2\pi i} \int_{\Gamma} \frac{a'(\lambda)}{a(\lambda)} d\lambda. \tag{9}$$

Obviously the number of breather pairs is then

$$N_{br} = \frac{1}{2}(N - N_s). \tag{10}$$

### III. EIGENVALUES FOR SYMMETRIC AND ANTISYMMETRIC BOXES

Here we consider initial disturbances which are piecewise-constant, and zero for  $x < -L_1$  and  $x > L_2$ . Note that then for a bound-state eigenfunction,  $\varphi_2(x) \equiv 0$  for  $x < -L_1$  and  $\varphi_1(x) \equiv 0$  for  $x > L_2$ . Recently Abdullaev and Tsoy<sup>11</sup> considered similar piecewise-constant initial disturbances in an analogous study of the initial-value problem for the Manakov system. Thus consider the rectangular well-like form illustrated in Fig. 2,

$$u(x) = \begin{cases} 0 & x < -L_1, \\ U_1 & -L_1 < x < 0, \\ U_2 & 0 < x < L_2, \\ 0 & L_2 < x. \end{cases} \tag{11}$$

To illustrate the exact results obtained for this initial condition, we also present several direct numerical simulations of the modified Korteweg–de Vries equation (1). These will show clearly the process of soliton and breather formation from rectangular well-like initial disturbances (11) as parameters are varied. A standard finite-difference scheme is applied.<sup>12</sup> The sides of the rectangular wells in the initial condition  $u(x)$  are smoothed in our simulations by replacing them with hyperbolic tangent functions with a width of 0.03, while the width of each peak in most experiments is approximately unity. Equation (1) is solved in a domain with width 40 and with zero boundary conditions. On the left boundary exponential dissipation is introduced to damp any reflection of the wave tail. The amplitude of the initial disturbance is allowed to vary.

In each region of the  $x$ -axis where the system (5) has constant coefficients, it is easily solved. At the boundaries between regions we require that both functions  $\varphi_1(x)$  and  $\varphi_2(x)$  should be continuous. It is then readily shown that the discrete spectrum for  $\mathcal{R}(\lambda) > 0$  satisfies the transcendental equation

$$\begin{aligned} & \left( \frac{\lambda + p_2}{U_2} - \frac{\lambda - p_1}{U_1} \right) (\lambda + p_1) e^{p_1 L_1 + p_2 L_2} \\ & + \left( \frac{\lambda - p_2}{U_2} - \frac{\lambda + p_1}{U_1} \right) (\lambda - p_1) e^{-p_1 L_1 - p_2 L_2} \\ & - \left( \frac{\lambda + p_2}{U_2} - \frac{\lambda + p_1}{U_1} \right) (\lambda - p_1) e^{p_2 L_2 - p_1 L_1} \\ & - \left( \frac{\lambda - p_2}{U_2} - \frac{\lambda - p_1}{U_1} \right) (\lambda + p_1) e^{p_1 L_1 - p_2 L_2} = 0, \end{aligned} \tag{12}$$

where

$$p_{1,2} = \sqrt{\lambda^2 - U_{1,2}^2}. \tag{13}$$

The magnitude of the variable  $p$  associated to a complex  $\lambda$  in this way is sometimes called the *quasimomentum*.

### A. Symmetric disturbances

First, to review known results in the context of our study, we consider a “single-peaked” disturbance ( $U_2 = 0, U_1 = U, L_1 = L$ ) which has of course a single polarity (positive for  $U > 0$ ). This special case of the potential pictured in Fig. 2 has been considered in detail by several authors;<sup>13,14</sup> see also Ref. 7 for a review. For this disturbance, (12) reduces to

$$\tanh(pL) = -\frac{p}{\lambda}, \tag{14}$$

where we have replaced  $p_1$  with  $p$ . Together with (13), the formula (14) enables us to find branches of the function  $\lambda(U)$  giving discrete eigenvalues of (5) as functions of the initial amplitude  $U$ . This set of equations can be represented in the parametric form,

$$|U| = \frac{p}{\sinh(pL)}, \quad \lambda = -p \coth(pL). \tag{15}$$

It is easily shown that the parameter  $p$  can only take imaginary values to satisfy the condition  $\mathcal{R}(\lambda) > 0$  and so there are only real eigenvalues, i.e., if  $\lambda$  belongs to the discrete spectrum of (5) for this potential, then  $\mathcal{I}(\lambda) = 0$ . It is then a discrete eigenvalue corresponding to a soliton of the modified Korteweg–de Vries equation. Introducing  $p = iy$ , the expression (15) becomes

$$|U| = \frac{y}{\sin(yL)}, \quad \lambda = -y \cot(yL). \tag{16}$$

There are an infinite number of branches, where each branch exists in the range

$$(2n + 1) \frac{\pi}{2} < yL < (n + 1) \pi, \tag{17}$$

for  $n = 0, 1, 2, 3, \dots$ . Note that the relation (16) is universal in the variables  $\lambda L$  and the mass,  $M = UL$ , and that it is sufficient to consider only the case  $U > 0$  as the case  $U < 0$  is obtained from antisymmetry. For large amplitudes of the initial disturbance the solution has the asymptotic form

$$\lambda_n(U) \approx U, \quad U \rightarrow \infty. \tag{18}$$

Each branch  $\lambda_n(U)$  begins from a critical value of the amplitude  $U = U_n^{(+)}$  given by

$$U_n^{(+)} = (2n + 1) \frac{\pi}{2L}, \tag{19}$$

near which the branch has the approximate form,

$$\lambda_n \approx U_n^{(+)} L (U - U_n^{(+)}), \quad U \rightarrow U_n^{(+)}. \tag{20}$$

Here the superscript (+) is meant to remind us that the total mass of  $u(x)$  is positive.

Thus, this rectangular-well disturbance of a single polarity has a discrete spectrum when  $U > \pi/2L$ , and the number of discrete eigenvalues is  $N$  where

$$N = \left\lfloor \frac{UL}{\pi} + \frac{1}{2} \right\rfloor, \tag{21}$$

where the braces denote the integer part. These results are similar to those obtained by Satsuma and Yajima<sup>9</sup> for the soliton-like initial disturbance  $u(x) = U \operatorname{sech}(x)$ , for which the eigenvalues of (5) are also purely real and are given exactly by

$$\lambda_n(U) = U - n + \frac{1}{2}. \tag{22}$$

Being real, each eigenvalue corresponds to the generation of a soliton with an amplitude

$$|A_n| = 2\lambda_n(U). \tag{23}$$

The soliton amplitude depends generally on both the height  $U$  of the rectangular well disturbance, and its length  $L$ . Due to (18) and (23) the amplitude of the generated soliton cannot exceed twice the height of the initial disturbance (as in the Korteweg–de Vries equation). As remarked earlier, the phase (location) of the soliton cannot be found from the corresponding eigenvalue alone; one must analyze the eigenfunctions to obtain this auxiliary spectral information. These results for the rectangular well are qualitatively similar to those for the soliton-like disturbance. The qualitative differ-

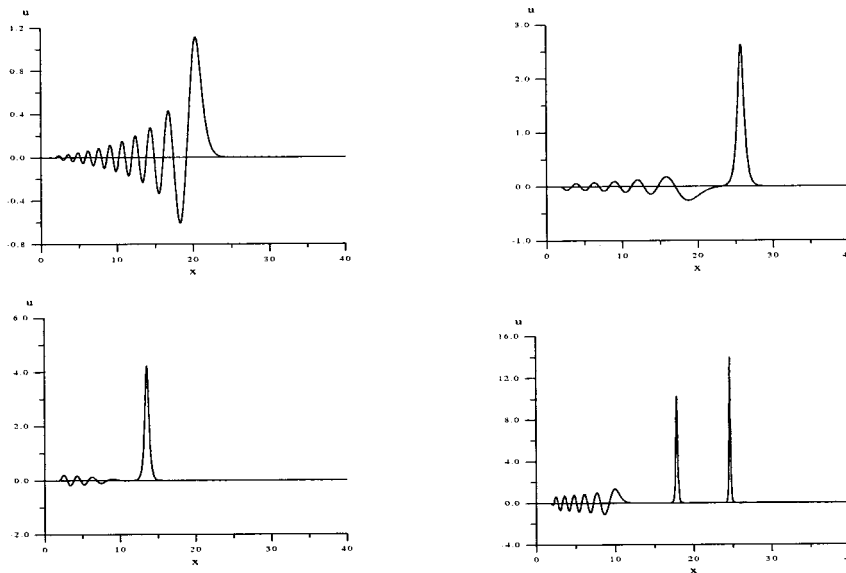


FIG. 3. Numerical simulations of the modified Korteweg–de Vries equation with positive square well initial data. Upper left:  $U=1.57$  and  $t=0.432$ . Upper right:  $U=2.5$  and  $t=0.7425$ . Lower left:  $U=\pi$  and  $t=0.135$ . Lower right:  $U=7.5$  and  $t=0.72$ .

ence between these initial conditions lies in the structure of the oscillatory tails. For instance, the soliton-like disturbance with mass  $M=UL=\pi$  will generate just one soliton (with no tail), because then its mass and energy are the same as for the soliton. But, the rectangular well disturbance with mass  $M=\pi$  will generate both a soliton and an oscillatory tail, because the energy of the generated soliton is less than the initial energy. We also want to point out that for strictly positive initial disturbances  $u(x)$ , it may be shown that the eigenvalues always emerge from the continuous spectrum at the origin  $\lambda=0$  as  $U$  increases; moreover the threshold condition  $a(0)=0$  can be computed exactly. (See Ref. 15 and references therein. Also, in the context of the application of the eigenvalue problem (5) to the undamped Maxwell–Bloch equations and the phenomenon of self-induced transparency, this result is connected with the McCall–Hahn ‘‘area theorem.’’<sup>13</sup>) This results in the exact statement that the  $n$ th eigenvalue appears when the mass integral is equal to

$$M = n\pi - \frac{\pi}{2}. \tag{24}$$

Each eigenvalue branch described above satisfies this exact threshold condition, as expected.

Representative snapshots of the numerical simulations of the evolution of a positive rectangular well disturbance of length  $L=1$  are shown in Fig. 3. In Eq. (11) we put  $U_2=0$  and  $L_1=1$ . The upper left-hand graph in Fig. 3 shows the evolution of a weak disturbance with amplitude  $U=1.57 < U_0^{(+)} = \pi/2$ . In the course of the evolution, the amplitude of the leading wave decreases, and an oscillatory tail is formed. For large times the tail begins to develop a self-similar oscillatory structure, which for sufficiently small amplitudes can be represented in terms of Airy functions. The upper right-hand graph in Fig. 3 shows the evolution of an initial disturbance with amplitude  $U=2.5$ . This disturbance evolves under (1) into one soliton and an oscillatory tail. The soliton amplitude is 2.6 as predicted by the spectral theory. Now, recall that an initial soliton-like disturbance with mass  $M=\pi$  evolves under (1) as a soliton with no oscillatory tail;<sup>9</sup>

an interesting contrast with this fact is illustrated in the lower left-hand graph of Fig. 3, where the initial amplitude of the square pulse was  $U=\pi$ , which implies that the mass is exactly  $\pi$ . This graph shows the evolution of the disturbance under (1) as a nonlinear superposition of a soliton and a dispersive oscillatory tail. This oscillatory tail compensates the deficit in energy between the rectangular initial disturbance and the exact soliton. Finally, the lower right-hand graph in Fig. 3 shows the evolution of a large disturbance, with  $U=7.5$ . In this case two solitons should form having amplitudes 14 and 10, according to the results of the spectral theory.

### B. Antisymmetric disturbances

Another special case treated in the literature is that of the piecewise-constant initial disturbance  $u(x)$  shown in Fig. 2 being antisymmetrical and therefore having zero total mass. We set  $U_2 = -U_1 = U$ ,  $L_2 = L_1 = L$ , so that

$$\int_{-\infty}^{+\infty} u(x) dx = 0. \tag{25}$$

This special case has been considered in Ref. 16 and also has been studied using an *ad hoc* variational approach in Ref. 17. Equation (12) for this potential reduces to the following parametric curve for  $p$  ( $p_1=p_2=p$  here),

$$\lambda^2 + \lambda p \coth(pL) + \frac{p^2}{2 \sinh^2(pL)} = 0, \tag{26}$$

with  $p$  being given by

$$p = \sqrt{\lambda^2 - U^2}. \tag{27}$$

It can be shown that there are no real solutions for  $\lambda$  of (26), and so this disturbance with zero mass cannot evolve as a nonlinear superposition of solitons (2). The eigenvalue  $\lambda$  (and therefore, the parameter  $p$ ) must be complex. Such complex solutions bifurcate from the continuous spectrum (the imaginary  $\lambda$ -axis) at the values given by

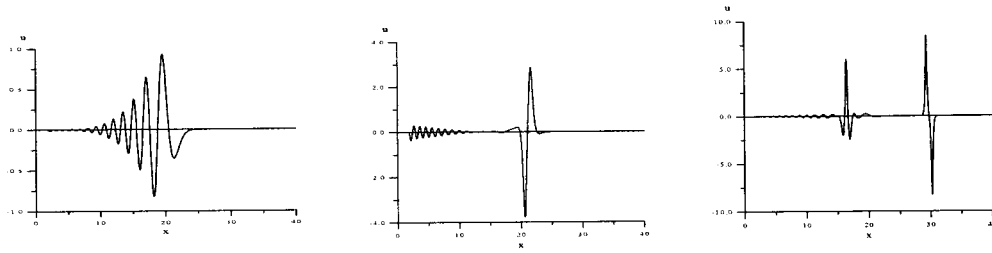


FIG. 4. Snapshots from three numerical simulations of the modified Korteweg–de Vries equation with “zero-mass” square well initial data. Left:  $U = 1$  and  $t = 0.1485$ . Middle:  $U = 2.5$  and  $t = 0.12$ . Right:  $U = 5$  and  $t = 0.126$ .

$$\lambda_n L = \pm \frac{i\pi}{2\sqrt{2}}(2n + 1), \tag{28}$$

and the bifurcations occur when  $U$  is tuned through the values  $U = U_n^{(0)}$  defined by

$$U_n^{(0)} L = \pm \frac{\pi}{2\sqrt{2}}(2n + 1). \tag{29}$$

The corresponding value of the parameter  $p$  is

$$p_n L = i y_n = \frac{i\pi}{2}(2n + 1). \tag{30}$$

Here, the superscript (0) in Eq. (29) refers to the potential  $u(x)$  having zero total mass. The solutions (28) of (26) correspond to spectral singularities of the eigenvalue problem (5) when  $U = U_n^{(0)}$ ; the so-determined values of  $\lambda$  are zeros of the function  $a(\lambda)$  (and so poles of the transmission coefficient) on the imaginary  $\lambda$ -axis. Note here the contrast with the situation for the KdV equation and for the mKdV equation with  $u(x) > 0$ . In those cases, the eigenvalue problem only admits spectral singularities at  $\lambda = 0$ , a distinguished point in the continuous spectrum.<sup>8</sup> As remarked earlier, such singularities are nongeneric and hence structurally unstable and expected to vanish under perturbation (e.g., small changes in the value of the amplitude parameter  $U$ ). The question is: when  $U$  is varied in the neighborhood of the bifurcation point  $U_n^{(0)}$ , does the spectral singularity disappear into the continuous spectrum, or emerge into the first quadrant of the  $\lambda$ -plane as a *bona fide* eigenvalue branch?

We choose to answer this question with perturbation analysis of the eigenvalue relation (26). Thus we seek a solution of (26) as a perturbation from the solution (28),

$$\lambda = \lambda_n + \delta\lambda, \quad U = U_n^{(0)} + \delta U, \quad p = p_n + \delta p. \tag{31}$$

At the first order of perturbation theory we obtain

$$\delta\lambda = \frac{\sqrt{2}y_n + i(1 - y_n^2/2)}{1 + y_n^2/2} \text{sign}(U_n^{(0)}) \delta U. \tag{32}$$

Here  $n = 0, 1, 2, 3, \dots$ . Because the eigenvalue condition (26) was derived assuming that  $\mathcal{R}(\lambda) \geq 0$ , we can only consistently admit solutions for which  $\mathcal{R}(\delta\lambda) \geq 0$ . Thus, this perturbation analysis establishes the existence of complex eigenvalues in the discrete spectrum as a bifurcation from the continuous spectrum (i.e., from the imaginary  $\lambda$ -axis), when

the amplitude *exceeds* the critical value (29). Each complex eigenvalue branch so obtained corresponds to the generation of a breather (4) in the course of the evolution under the modified Korteweg–de Vries Eq. (1) from the zero-mass initial condition  $u(x)$ . The first breather is generated when the amplitude  $U$  exceeds the first critical value  $U_0^{(0)} = \pi/2\sqrt{2}L \approx 1.11/L$ , the second at  $3U_0^{(0)}$ , and so on. Here we assume without any loss of generality that  $U > 0$ . If  $U < U_0^{(0)}$  then there are no discrete eigenvalues whatsoever and consequently only a dispersive oscillatory tail is formed during the evolution. It is important to note that for large amplitudes  $U$  (we can take  $U > 0$  without loss of generality) of the initial disturbance,  $\mathcal{R}(\lambda)$  has the asymptotic value (18), and  $\mathcal{I}(\lambda)$  tends to zero. An “almost” real value for the eigenvalue means that the corresponding breather (4) will resemble a nonlinear superposition of a pair of solitons (2) of the same amplitude but opposite polarities over long time intervals, with a weak interaction between them. We call this situation a *quasistationary coupled soliton pair*.

The process of breather formation from a rectangular well initial disturbance, with both polarities and zero mass, (i.e.,  $U_1 = -U_2 = U, L_1 = L_2 = 1$ ) is illustrated with three snapshots of numerical simulations of the modified Korteweg–de Vries equation in Fig. 4. The left-hand plot is a snapshot of the evolution for an initial disturbance with  $U < U_0^{(0)}$  that is not sufficiently energetic to generate any breathers at all. The plot in the middle of Fig. 4 shows a snapshot from an evolution for  $U_0^{(0)} < U < 2U_0^{(0)}$  for which one breather forms. Finally, in the right-hand plot of Fig. 4, we present the results of an evolution for  $2U_0^{(0)} < U < 3U_0^{(0)}$  when two breathers are generated. In each case, the number of breathers is in full agreement with the above analysis. Also, the numerical simulations confirm that no solitons form in this case.

#### IV. TRANSITION FROM SOLITONS TO BREATHERS FOR BOX INITIAL CONDITIONS

The bifurcation of a complex conjugate pair into a real pair or vice versa can occur as the potential is continuously tuned through a physically reasonable family. To illustrate this phenomenon, and to appreciate the complexity of the eigenvalue problem (5), we study the general potential (11) numerically. That is, we explicitly write down the eigenvalue condition  $a(\lambda) = 0$ , which for the potential (11) has an obvious analytic continuation into the right half-plane [ $\mathcal{R}(\lambda)$

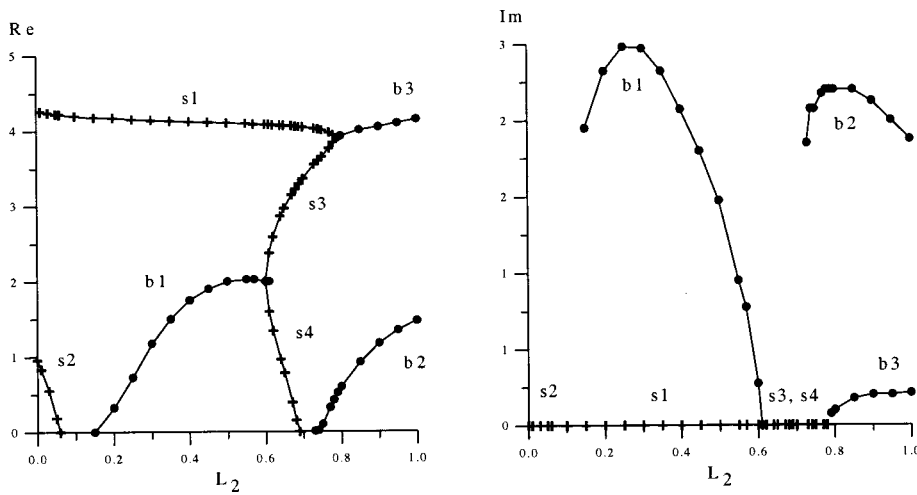


FIG. 5. The discrete spectrum (here complex-valued) for the rectangular well disturbance. Here  $U_1 = -U_2 = 5$ ,  $L_1 = 1$ , and  $L_2$  is varied. Left: the real parts of the eigenvalues as functions of  $L_2$ . Right, the corresponding imaginary parts.

$\geq 0$ ] and then we use a numerical root-finding procedure to find solutions of this equation in the complex plane for different values of the potential parameters. Here we study in detail the discrete spectrum for the two-peaked disturbance  $u(x)$  with opposite polarities given by (11) with parameters  $U = U_1 = -U_2 = 5$ ,  $L_1 = 1$ , and then we allow  $L_2$  to vary between zero and  $L_1$ . Therefore, we are now providing new detailed results that interpolate between the two cases previously studied in the literature and reviewed in Sec. III. According to the analytical results when  $L_2 = 0$ , there are two real discrete eigenvalues in the spectrum, but when  $L_2 = L_1$  there should be two complex pairs of eigenvalues. The numerical root-finding results we now describe tune continuously between these two limiting cases.

The results of our calculations are presented in Fig. 5. For small  $L_2$  we have two real eigenvalues (which we label as  $s_1$  and  $s_2$ ), representing two solitons, as for  $L_2 = 0$ . As  $L_2$  increases, the second real eigenvalue,  $s_2$ , decreases and disappears into the continuous spectrum at  $L_2 = 0.05$ . For  $0.05 < L_2 < 0.15$  we have only one real eigenvalue,  $s_1$ , representing just one soliton. For  $L_2 = 0.15$  a complex eigenvalue (labeled as  $b_1$ ) is born, corresponding to a breather. It emerges into the first quadrant from the imaginary  $\lambda$ -axis with a finite imaginary part. In between the disappearance of  $s_2$  and the appearance of  $b_1$ , there are no spectral singularities (embedded eigenvalues) in the continuous spectrum, so it is not clear if in any sense the breather  $b_1$  is a continuation of the

soliton branch  $s_2$ . Next, this complex eigenvalue,  $b_1$ , coalesces with its complex-conjugate on the real axis at  $L_2 = 0.6$  and the double eigenvalue that results unfolds for  $L_2 > 0.6$  as a pair of distinct real eigenvalues (labeled  $s_3$  and  $s_4$ ). This is exactly the phenomenon we mentioned earlier, with the bifurcation happening at a certain structurally unstable potential  $u(x)$ . At this point in the tuning of the parameter  $L_2$ , we now have three real eigenvalues ( $s_1$ ,  $s_3$ , and  $s_4$ ) and the corresponding initial disturbance should evolve under the modified Korteweg–de Vries equation (1) into three solitons. However, when  $L_2$  is further increased to  $L_2 = 0.68$ , the real eigenvalue  $s_4$  disappears, being absorbed into the continuous spectrum at  $\lambda = 0$ . The next bifurcation occurs when  $L_2 = 0.73$ , at which point a new complex eigenvalue, labeled  $b_2$ , is born, again from the imaginary axis with a finite imaginary part. At  $L_2 = 0.79$  the two remaining real eigenvalues ( $s_1$  and  $s_3$ ) coalesce and the double eigenvalue is unfolded for slightly larger  $L_2$  as another complex eigenvalue,  $b_3$ , (and its complex conjugate). Finally, as  $L_2 \rightarrow 1$  we have the two complex eigenvalues ( $b_2$  and  $b_3$ ) only, in agreement with the previous analysis. This example shows quite a complicated picture of eigenvalue behavior and bifurcation, even for this relatively simple form of the initial disturbance (11), and we infer that there will be a corresponding complicated pattern of soliton and breather formation under the evolution of the modified Korteweg–de Vries equation (1) as parameters are varied.

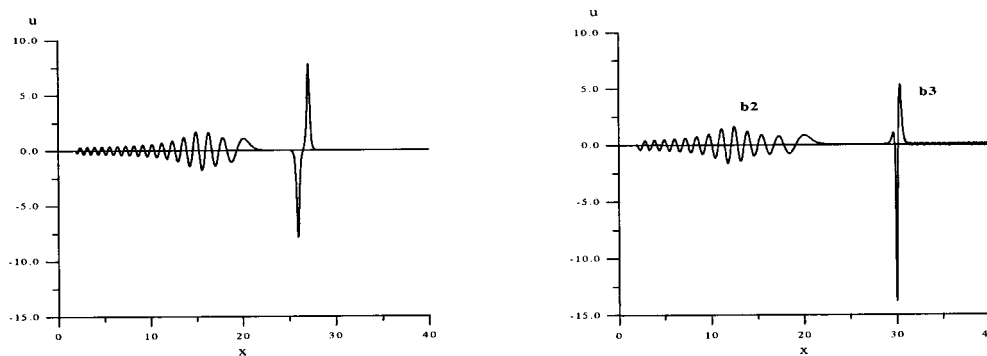


FIG. 6. The evolution of a two-peaked initial disturbance with  $U_1 = -U_2 = 5$ ,  $L_1 = 1$ , and  $L_2 = 0.8$ . Left:  $t = 0.09$ . Right:  $t = 0.1485$ .

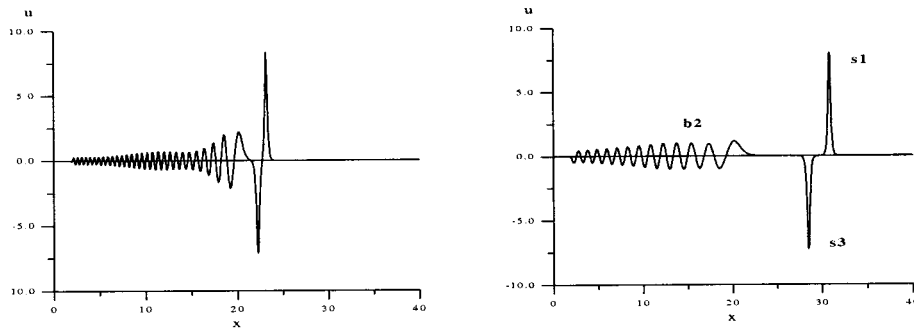


FIG. 7. The evolution of a two-peaked initial disturbance with  $U_1 = -U_2 = 5$ ,  $L_1 = 1$ , and  $L_2 = 0.75$ . Left:  $t = 0.03$ . Right:  $t = 0.1485$ .

Again using numerical simulations of (1), we illustrate the intermediate regimes of breather and soliton generation by using the parameter  $L_2$  to tune between the strictly positive and zero-mass cases. In these numerical simulations the rectangular well disturbance is represented by a (smoothed) two-peaked form as in Fig. 2, with heights  $U = U_1 = -U_2 = 5$ ,  $L_1 = 1$ , while  $L_2$  is varied between  $L_2 = 0$  and  $L_2 = 1$ . If  $L_2 = L_1 = 1$ , we have a case of an initial disturbance with zero mass, and it corresponds to the generation of two breathers, b2 and b3. This scenario of the generation of two breathers is maintained at first as  $L_2$  decreases, but when  $L_2 = 0.8$  one of the breathers (b2) has a very small amplitude, and a simulation corresponding to this case is shown in Fig. 6. When the length parameter has decreased to  $L_2 = 0.75$  the larger, leading breather (b3) has transformed into two solitons (s1 and s3) of opposite polarity with nearly equal amplitudes as shown in Fig. 7. This bifurcation is exactly as predicted by the spectral theory, namely the coalescence of the complex eigenvalue corresponding to b3 with its complex conjugate, resulting in the two real eigenvalues corresponding to the solitons s1 and s3. Decreasing  $L_2$  through the range  $0.6 < L_2 < 0.68$ , a third soliton (s4) has been generated, and a snapshot from a corresponding simulation showing the presence of this soliton is shown in Fig. 8. When  $L_2 = 0.5$ , the two solitons s3 and s4 have combined and merged to become the breather b1; a numerical simulation corresponding to this case is shown in Fig. 9. When the length has been tuned down to  $L_2 = 0.2$  the breather has become much more oscillatory and very small in amplitude; its eigenvalue quartet is on the verge of vanishing into the continuous spectrum (at which point its energy will be converted into dispersive radiation). The corresponding simulation is shown in Fig. 10. Finally when  $L_2 < 0.1$  the breather has vanished and a new

soliton s2 has emerged from the continuous spectrum. At this point the evolution is similar to that illustrated in the lower right-hand graph of Fig. 3. The sequence of wave transformations illustrated in this sequence of numerical experiments corresponds exactly to the bifurcation of eigenvalues that occurs with decreasing  $L_2$  as described above.

The formulas (8), (9), and (10) can be used to independently verify that the numerical root-finding procedure has found all of the eigenvalues in the right half-plane. Moreover, if we are only concerned with the number of eigenvalues, these formulas can be used to further put into context the sequence of bifurcations shown in Fig. 5. To do this it is most convenient to let  $U_1 = -U_2 = U$ ,  $L_1 = 1$  and allow the mass and energy of the initial disturbance to be varied, where the energy of a disturbance is

$$E = \frac{1}{2} \int_{-\infty}^{\infty} u^2(x) dx. \tag{33}$$

The mass and energy are then  $M = U(1 - L_2)$  and  $E = \frac{1}{2}U^2(1 + L_2)$ . The plots in Fig. 11 show the numbers of eigenvalues corresponding to solitons and breathers over a whole region of the  $(M, E)$  plane. Along the dotted line in Fig. 11,  $U = 5$  and  $L_2$  increases from 0 at  $E = \frac{1}{2}M^2$  to 1 at  $M = 0$ . Comparing this with Fig. 5, and keeping in mind that a breather corresponds to a pair of conjugate eigenvalues in the right half-plane while a soliton corresponds to a single real eigenvalue in the right half-plane, we see that all eigenvalues in the discrete spectrum have been captured in Fig. 5 over the whole range of the parameter  $L_2$ .

A comparison of Fig. 5 and Fig. 11 demonstrates that the onset of the branches s4 and s2 corresponds to the emergence of a soliton eigenvalue out of the continuous spectrum as the

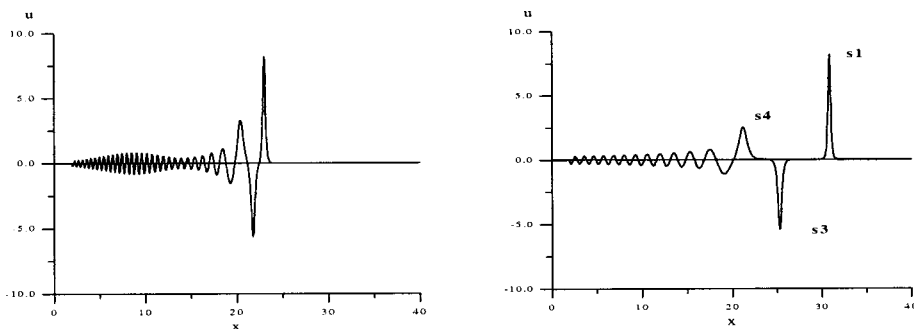


FIG. 8. The evolution of a two-peaked initial disturbance with  $U_1 = -U_2 = 5$ ,  $L_1 = 1$ , and  $L_2 = 0.63$ . Left:  $t = 0.03$ . Right:  $t = 0.1485$ .



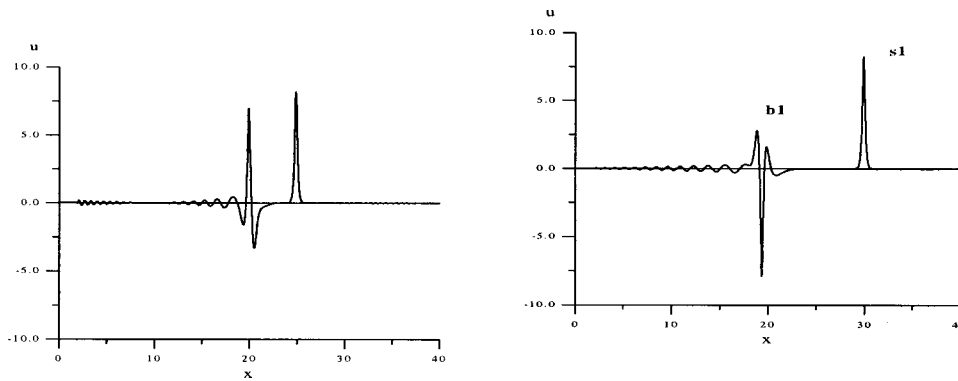


FIG. 9. The evolution of a two-peaked initial disturbance with  $U_1 = -U_2 = 5$ ,  $L_1 = 1$ , and  $L_2 = 0.5$ . Left:  $t = 0.06$ . Right:  $t = 0.135$ .

mass increases through the threshold values  $\pi/2$  and  $3\pi/2$ , respectively, in agreement with (24). Indeed the only unique lines on the soliton eigenvalues plot of Fig. 11 are those for which  $M = \pi/2$  and  $3\pi/2$ , with all other curves also occurring in the breather eigenvalue pairs plot. Therefore bifurcations of solitons from the continuous spectrum only occur at these threshold values of the mass. However, as the mass of the initial disturbance is increased these bifurcations can correspond to either the emergence of a soliton from the continuous spectrum or the subsuming of a soliton into the continuous spectrum. *This result shows that the intuition that a soliton should emerge from  $\lambda = 0$  at the thresholds as the mass is increased is patently false.* As the mass increases, these transitions which occur for all real-valued potentials and are characterized generally in terms of the mass integral by (24), can correspond to *either* soliton birth or soliton death events.

All the curves of the left-hand plot of Fig. 11, except for  $M = \pi/2$  and  $3\pi/2$  and  $2E = M^2$  correspond to bifurcations of breather eigenvalue pairs from the continuous spectrum. Here the more common occurrence is that as the mass is increased breather eigenvalue pairs are subsumed into the continuous spectrum, although as with the soliton eigenvalues the opposite can also occur.

In general we can state that for initial disturbances with large mass and energy, i.e., close to  $2E = M^2$ , the generation of solitons will be favored. Conversely, for disturbances with small mass, but finite energy, i.e., close to  $M = 0$ , the generation of breathers is favored. Indeed, for the two-peak initial

disturbance considered here solitons are not generated for  $M \leq 0.5$ . Between these two limits a complicated pattern of bifurcations occurs and no general statement can be made for an arbitrary initial disturbance.

### V. CONCLUSIONS

In this article, we have studied the initial-value problem for the modified Korteweg–de Vries equation (1) with a positive coefficient for the cubic nonlinear term (so the equation admits solitons) using both analytical methods based on the AKNS system (5) for the inverse scattering method, and direct numerical simulations. Our aim has been to determine the kinds of initial disturbance which can lead to solitons on the one hand, and breathers on the other. We have confined our study to piecewise-constant initial conditions for analytical convenience, but would claim that the conclusions drawn from these cases are representative of more general initial conditions.

Solitons correspond to real-valued eigenvalues in the discrete spectrum of the AKNS system, and are typically generated by initial disturbances of a dominant polarity and sufficient mass. On the other hand, breathers correspond to complex-valued eigenvalues, and are typically generated by initial disturbances with very small mass and sufficient energy. Further we have shown that breathers can either be generated by coincident solitons of opposite polarities (i.e., a quasistationary coupled soliton pair), corresponding to a complex unfolding of a double real eigenvalue, or can

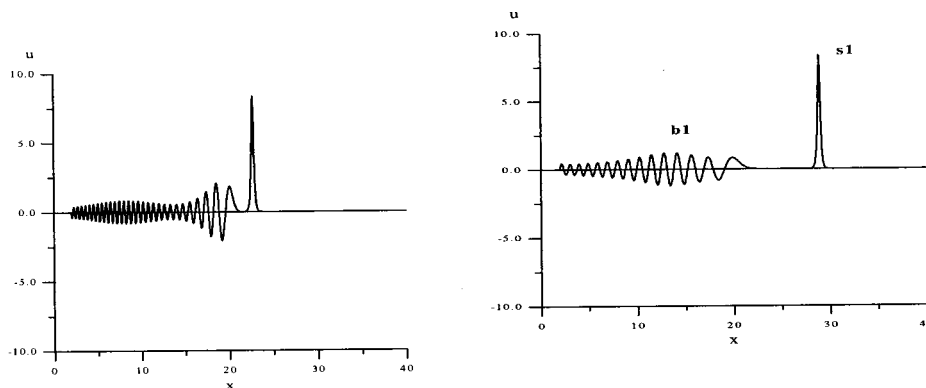


FIG. 10. The evolution of a two-peaked initial disturbance with  $U_1 = -U_2 = 5$ ,  $L_1 = 1$ , and  $L_2 = 0.2$ . Left:  $t = 0.03$ . Right:  $t = 0.1485$ .

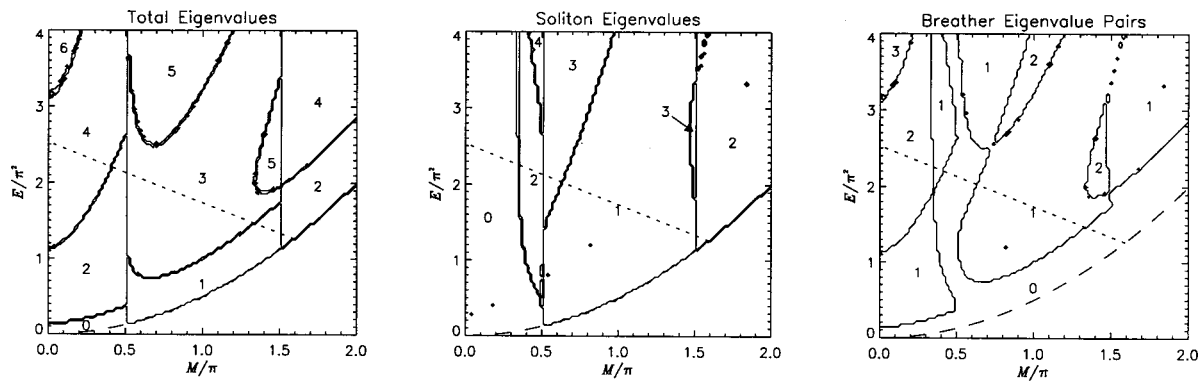


FIG. 11. The number of eigenvalues as a function of the mass and energy for the two-peaked initial disturbance with  $U_1 = -U_2 = U$  and  $L_1 = 1$ . The total number of eigenvalues, number of soliton eigenvalues, and number of breather eigenvalue pairs are given by the formulas (8), (9), and (10). The numbers of eigenvalues in each plot is only calculated above the dashed curve  $E = \frac{1}{2}M^2$ , upon which  $L_2 = 0$ . The dotted line corresponds to  $U = 5$ , for which the eigenvalue bifurcations are shown in Fig. 5.

emerge spontaneously from the continuous spectrum as a bifurcation of a zero of the reciprocal  $a(\lambda)$  of the transmission coefficient.

Our direct numerical simulations of the modified Korteweg–de Vries equation show in detail the formation of both breathers and solitons, together with an oscillatory tail, in good agreement with our analysis and the consequent theoretical predictions. As a final remark, we want to emphasize again that all of our statements concerning eigenvalues of the scattering problem (5) also immediately imply analogous facts for the initial-value problem for all commuting flows (e.g., nonlinear Schrödinger, sine-Gordon, etc.).

## ACKNOWLEDGMENTS

Simon Clarke and Roger Grimshaw acknowledge the Australian Research Council under Grant No. A89800458. Peter Miller was supported by a Monash University Logan Fellowship. Efim Pelinovsky and Tatiana Talipova were supported by RFBR under Grant No. 99-05-65576, by the Australian Research Council under Grant No. A39702096, and by INTAS under Grant No. 99-1068. The authors would like to thank D. Pelinovsky and V. E. Zakharov for useful comments and pointing our attention to a number of relevant references.

<sup>1</sup>T. Perelman, A. Fridman, and M. El'yashevich, "A modified Korteweg–de Vries equation in electrodynamics," *Sov. Phys. JETP* **39**, 643–646 (1974).

<sup>2</sup>E. Pelinovsky and V. Sokolov, "Nonlinear theory for the propagation of electromagnetic waves in size-quantized films," *Radiophys. Quantum Electron.* **19**, 378–382 (1976).

<sup>3</sup>R. Grimshaw, E. Pelinovsky, and T. Talipova, "The modified Korteweg–de Vries equation in the theory of large-amplitude internal waves," *Nonlinear Processes in Geophysics* **4**, 237–250 (1997).

<sup>4</sup>T. Talipova, E. Pelinovsky, K. Lamb, R. Grimshaw, and P. Holloway, "Cubic nonlinearity effects at the intense internal wave propagation," *Trans. Russ. Acad. Sci., Earth Section* **364**, 824–827 (1999).

<sup>5</sup>I. S. Pavlov, *Quasiplane Waves in Two-dimensional Elastic System*, in *Physical Technologies in Industry* (Nizhny Novgorod, 1998), pp. 18–21.

<sup>6</sup>G. L. Lamb, *Elements of Soliton Theory* (Wiley, New York, 1980).

<sup>7</sup>R. K. Dodd, J. C. Eilbeck, J. D. Gibbon, and H. C. Morris, *Solitons and Nonlinear Wave Equations* (Academic, London, 1982).

<sup>8</sup>P. G. Drazin and R. S. Johnson, *Solitons: An Introduction* (Cambridge University Press, Cambridge, England, 1993).

<sup>9</sup>J. Satsuma and N. Yajima, "Initial value problems of one-dimensional self-modulation of nonlinear waves in dispersive media," *Suppl. Prog. Theor. Phys.* **55**, 284–306 (1974).

<sup>10</sup>Z. V. Lewis, "Semiclassical solution of the Zakharov–Shabat scattering problem for phase-modulated potentials," *Phys. Lett.* **112A**, 99–103 (1985).

<sup>11</sup>F. Kh. Abdullaev and E. N. Tsoy, "The evolution of two optical beams in self-focusing media," *Physica D* (submitted).

<sup>12</sup>Yu. A. Berezin, *Modeling Nonlinear Wave Processes* (VNU Science, Utrecht, 1987).

<sup>13</sup>D. J. Kaup, "Coherent pulse propagation: A comparison of the complete solution with the McCall–Hahn theory and others," *Phys. Rev. A* **16**, 704–719 (1977).

<sup>14</sup>J. Burzlaff, "The soliton number of optical soliton bound states for two special families of input pulses," *J. Phys. A* **21**, 561–566 (1988).

<sup>15</sup>M. Desaix, D. Anderson, M. Lisak, and M. L. Quiroga-Teixeiro, "Variationally obtained approximate eigenvalues of the Zakharov–Shabat scattering problem for real potentials," *Phys. Lett. A* **212**, 332–338 (1996).

<sup>16</sup>D. J. Kaup and L. R. Scaccia, "Generation of  $0\pi$  pulses from a zero-area pulse in coherent pulse propagation," *J. Opt. Soc. Am.* **70**, 224–230 (1980).

<sup>17</sup>D. J. Kaup and B. A. Malomed, "Variational principle for the Zakharov–Shabat equations," *Physica D* **84**, 319–328 (1993).